

See discussions, stats, and author profiles for this publication at: <https://www.researchgate.net/publication/338397745>

# Solar Sailing Fundamentals with an Exploration of Trajectory Control to Lunar Halo Orbit

Conference Paper · January 2020

DOI: 10.2514/6.2020-1207

CITATIONS

0

READS

17

3 authors:



**Leonard Vance**

The University of Arizona

15 PUBLICATIONS 27 CITATIONS

SEE PROFILE



**Ravi Teja Nallapu**

The University of Arizona

45 PUBLICATIONS 161 CITATIONS

SEE PROFILE



**Jekan Thangavelautham**

The University of Arizona

205 PUBLICATIONS 834 CITATIONS

SEE PROFILE

Some of the authors of this publication are also working on these related projects:



On-Orbit Centrifuge Laboratory [View project](#)



Robotics and Neural Networks [View project](#)

See discussions, stats, and author profiles for this publication at: <https://www.researchgate.net/publication/337696978>

# Solar Sailing Fundamentals with an Exploration of Trajectory Control to Lunar Halo Orbit

Article in *Collection of Technical Papers - AIAA/ASME/ASCE/AHS/ASC Structures, Structural Dynamics and Materials Conference* · December 2019

CITATIONS

0

READS

42

## 3 authors:



**Leonard Vance**

The University of Arizona

15 PUBLICATIONS 26 CITATIONS

[SEE PROFILE](#)



**Ravi Teja Nallapu**

The University of Arizona

44 PUBLICATIONS 154 CITATIONS

[SEE PROFILE](#)



**Jekan Thangavelautham**

The University of Arizona

202 PUBLICATIONS 802 CITATIONS

[SEE PROFILE](#)

Some of the authors of this publication are also working on these related projects:



Fuel Cells for Robots and Mobile Devices [View project](#)



Space Missions [View project](#)

# Solar Sailing Fundamentals with an Exploration of Trajectory Control to Lunar Halo Orbit

Leonard D. Vance\* and Ravi teja Nallapu †  
*University of Arizona, Tucson, AZ-85719.*

Jekanthan Thangavelautham‡  
*University of Arizona, Tucson, AZ-85719.*

**This paper covers the basic physics of solar sailing and then explores practical guidance techniques for controlling solar sailing spacecraft on the earth-moon halo orbit entry manifolds expected to be used by NASA’s Lunar Gateway. A four body (Sun, Earth, Moon, spacecraft) simulation is utilized to generate the resultant trajectory performance. Biases to the reference manifold trajectories are derived to center spacecraft acceleration capability within the limited solar sailing acceleration envelope, and improvements in performance are demonstrated.**

## I. Introduction

The decision to place the Lunar Gateway space station in a low energy halo orbit provides an opportunity to implement orbit transfers from low Earth to Lunar Gateway halo orbit using only solar pressure. The possibility of effecting transfers to the moon without propellant could significantly improve the mass rate delivery to the proposed Gateway. The derivation of manifolds (or reference trajectories) leading to stable Earth-Moon halo orbits provides mission designers with opportunities to enter these orbits at a conveniently significant distance from the final destination where disturbances from the moon are less noticeable. In the case of the proposed Lunar Gateway orbit, the manifold propagates all the way to the opposite side of the earth-moon system. The existence of these low velocity trajectories offers the possibility of being able to access the lunar gateway orbit with very low thrust systems such as a solar sailcraft.

## II. Reference Manifolds to Halo Orbits

This section describes the algorithm to construct the reference manifold trajectories, that the solar sailing spacecraft tracks in order to be captured onto the desired halo orbits. We assume that the reference trajectory obeys the circular restricted three body problem (CR3BP) dynamics [1]. The halo orbits show up as non-planar periodic trajectories in the vicinity of the colinear libration points when the CR3BP dynamics are assumed [2]. A stable manifold of a halo orbit is a trajectory in the phase space of CR3BP, where a spacecraft placed on any point on this trajectory will end up being captured by the corresponding halo orbit [3]. Here, we present a brief overview of construction of a halo orbit, and its corresponding stable manifold.

### A. Halo Orbit Generation

In this work, we employ a single shooting differential corrector to construct these halo orbits [4]. The differential corrector requires an initial guess for the orbital period  $T'_p$ , and initial conditions  $R'_0$ . These guesses are then iteratively corrected using the state transition matrix (STM), denoted by  $\Phi(R_0, t_0, t_f)$ . The STM is a linear mapping of a point  $R_0$  in the phase space, starting at  $t_0$ , to its end point at  $t_f$ . Exploiting the symmetry of the halo orbits, the initial guess for a halo orbit can be written as

$$R'_0 = \begin{bmatrix} x'_0 & 0 & z'_0 & 0 & v'_{y,0} & 0 \end{bmatrix}^T \quad (1)$$

Note the superscript ' denotes that the parameter is an initial guess. The values of  $z'_0$ ,  $v'_{y,0}$ , and  $T'_p$  are then corrected based on the values of  $x$ , and  $z$  component velocities at the end of half period  $T'_p/2$ . The STM  $\Phi(R'_0, 0, T'_p/2)$  is used

---

\*Ph.D. Student, Aerospace Engineering, ldvance@email.arizona.edu.

†Ph.D. Candidate, Aerospace Engineering, rnallapu@email.arizona.edu

‡Assistant Professor, Aerospace and Mechanical Engineering Department, jekan@email.arizona.edu.

to correct the values of  $z'_0$ ,  $v'_{y,0}$ , and  $T'_p$  at every step of the iteration. The end result of the differential correction process is a periodic trajectory which starts at an initial condition specified by Equation 2, and after a period of  $T_p^*$  returns to the same initial condition within some user specified tolerance, along with the history of the spacecraft trajectory during the time  $0 \leq t \leq T_p^*$ .

$$R_0^* = \begin{bmatrix} x'_0 & 0 & z'_0 & 0 & v_{y,0}^* & 0 \end{bmatrix}^T \quad (2)$$

Note that the superscript  $'$  in Equation 1 denotes a guess, while the superscript  $*$  in equation 2 denotes that the parameter indicates that the parameter is used for generating the halo orbit. The other result of the differential correction is the state transition matrix at the end of the orbital period  $T_p^*$  which is referred to as the monodromy matrix  $\Phi_M$ , i.e.,

$$\Phi_M = \Phi(R_0^*, 0, T_p^*) \quad (3)$$

As described above, the halo orbit generation algorithm is highly sensitive to the initial guess of  $R'_0$ , and  $T'_p$ . In this work we use a catalog of halo orbit initial conditions as described in [5], which is then supplied to the differential corrector algorithm. The catalog is constructed based on the conditions presented in [4]. Such catalogs allow us to parameterize the halo orbits using an integer index  $i$ , which corresponds to the initial guess for the initial conditions and orbital period.

## B. Stable Manifold Generation

The stable manifolds of a halo orbit serve as ballistic transport trajectories on to the corresponding halo orbit. A manifold can be generated by selecting a point on the manifold, where the spacecraft would theoretically enter onto the manifold. This is achieved by discretizing the time history of the halo orbit as shown in Figure 1. In this work, we use a uniform time based sampling scheme is used to generate  $N_E$  discrete points on the halo orbit, which serve as the entry point on the manifold. From this sample we select a an entry point specified by index  $j$ , such that  $1 \leq j \leq N_E$ . Following this we apply the accelerated manifold construction strategy described in [6] to construct the transfer manifold. The manifold construction algorithm can be described as follows.

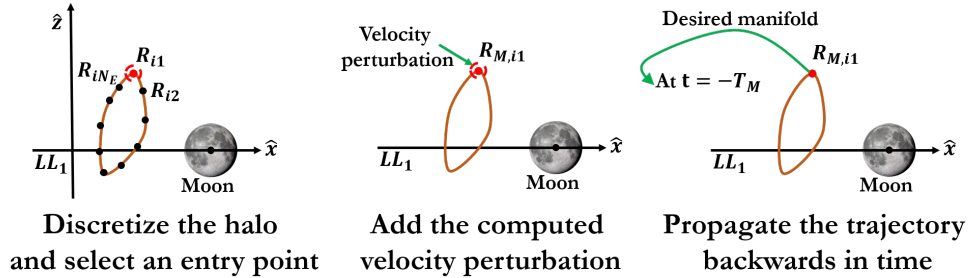


**Fig. 1** An illustration of the different steps required to construct stable accelerated halo manifolds

Let  $R_{j/i}$  correspond to the selected phase space entry point  $j$  on the  $i^{th}$  halo orbit. The monodromy matrix of this halo orbit  $\Phi_{M,i}$  is characterized by stable, center, and unstable sub spaces. Let  $V_1^S$ , and  $V_2^S$  denote the normalized eigen vectors corresponding to the stable eigen values  $\lambda_1^S$ , and  $\lambda_2^S$  of the monodromy matrix respectively. We note that the eigen vectors can be formatted as

$$V_{1,2}^S = \begin{bmatrix} r V_{1,2}^S \\ v V_{1,2}^S \end{bmatrix} \quad (4)$$

Where  $r V_{1,2}^S$  corresponds to a  $3 \times 1$  vector which forms the position component of the corresponding eigen vector, and  $v V_{1,2}^S$  forms its velocity component. Noting that the components of these eigen vectors are complex conjugates of each other, we can defined a point on the accelerated manifold as

$$R_{M.,j/i} = R_{j/i} + d \left( \begin{bmatrix} 0 \\ vV_1^S \end{bmatrix} + \begin{bmatrix} 0 \\ vV_2^S \end{bmatrix} \right) \quad (5)$$

Where  $d$  is a small perturbation selected. A value of  $d = 50$  km is commonly used for the Earth-Moon system. This trajectory is then propagated backwards in time from 0 to  $-T_M$  to generate the manifold. This allows us to parameterize the manifold of a halo orbit using the indices  $i, j$  and the back propagation time  $T_M$ . The accelerated manifold generation process is summarized in Figure 1.

### III. Solar-sail Spacecraft Performance

Available accelerations for a solar sailcraft are very low, even for aggressive mass reduction assumptions. The spacecraft assumed for the purpose of this paper is based upon the Planetary Society's Lightsail 2 spacecraft, but with acceleration capability increased to 0.0028 m/s<sup>2</sup> for the exploratory purposes of this paper.

The reference manifolds described earlier in this paper provide a theoretical set of trajectories which lead to a final stable halo orbit, but only in a restricted three body problem where the two bodies producing gravity are in circular orbits around the mutual center of gravity. In actuality, the earth moon system has an eccentricity close to 0.03, which means the distance to the moon fluctuates significantly relative to these ideal solutions, plus the sun produces its own influence, which further influences the trajectory of a spacecraft outside the idealized calculated manifold.

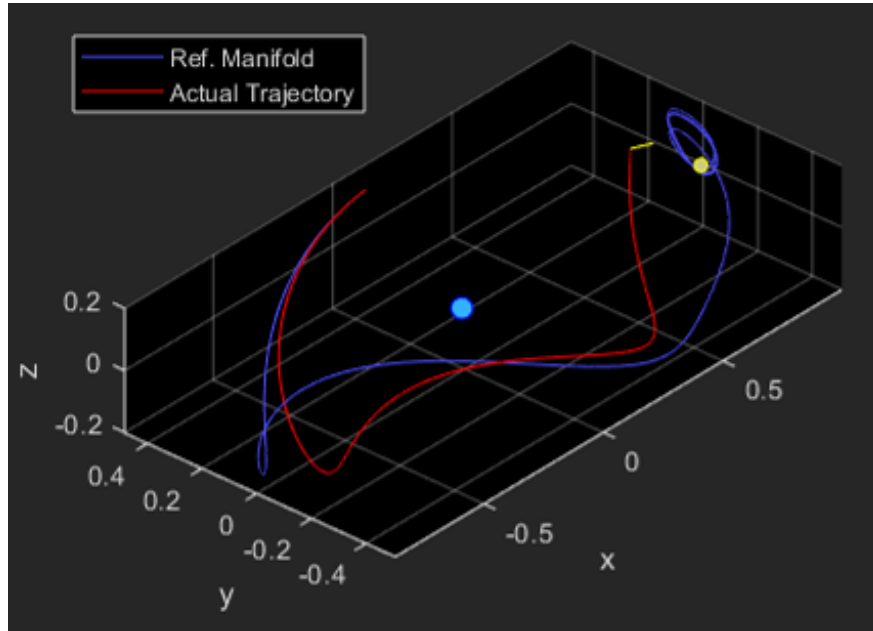


**Fig. 2 The reference manifold trajectory generated from the restricted 3 body problem shows significant deviation when executed in a four body simulation**

A four-body simulation approach (Sun, Earth, Moon, spacecraft) is used in this paper to calculate spacecraft trajectories and the resulting motion is viewed in the relative line of sight frame between the earth and the moon for the sake of convenience. Initial conditions for the Earth and Moon are taken from the New Horizons website for the Julian date of 2458849.5 (Jan 01 2020, 0000hrs UTC).

#### A. Limitations of the Restricted Three Body Approach

Figure 2 shows a reference input manifold for the Lunar Gateway orbit consistent from the restricted 3 body problem solution described in II. Superimposed over this is the four-body simulated trajectory of a spacecraft initialized using that manifold's initial calculation for position and velocity. Most papers on this subject, such as [7] work this problem from

the restricted 3 body problem, but the effects of the earth-moon eccentricity along with solar gravity are immediately apparent, with the error in final position more than 0.4 earth-moon distances after a 24 day propagation.

In order to successfully guide to the final halo orbit, we must either establish manifolds which include the four body effects, and/or design a controller which overcomes these disturbances and holds the spacecraft on the reference manifold. Because any practical application must include a control algorithm of some type for guidance, this approach is implemented with the intent of adapting it to a solar sailing spacecraft.

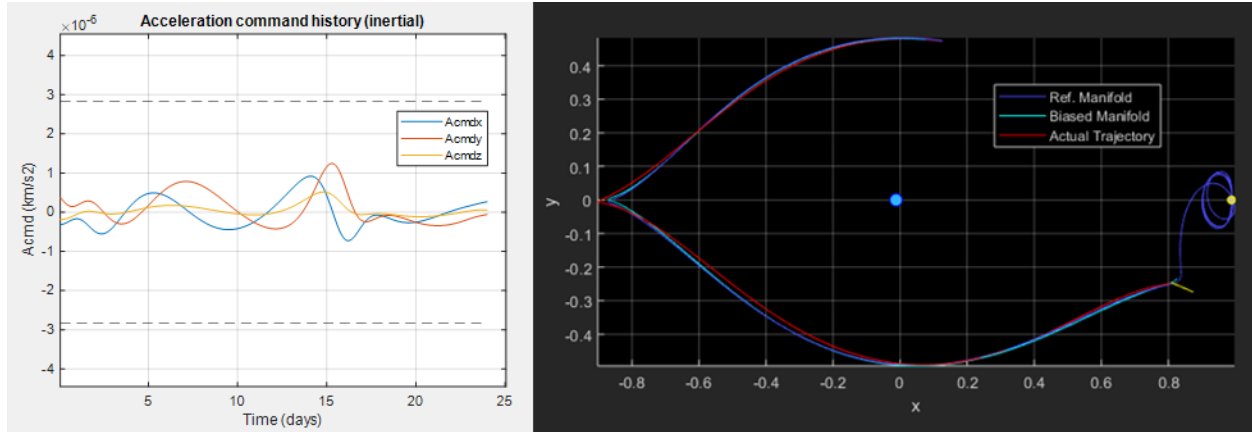


**Fig. 3 A PID controller produces good trajectory control with acceleration limits consistent with solar sail acceleration capability**

A three axis PID control algorithm is applied to the spacecraft, with position and velocity errors relative to the reference manifold trajectory. A forward feed integrator is added to eliminate position steady state error. The resultant trajectory (figure 3) follows the reference manifold easily with acceleration commands which are within the capability of assumed solar sail spacecraft. This implies that this control law can now be adapted for solar sailing.

### B. Overview of Solar Sailing

A solar sailcraft utilizes the pressure exerted on a thin reflecting membrane from a light source such as the Sun (in this case). By tilting the sail with respect to the light source, the resultant thrust can be directed laterally to some extent, with some limited response available within the entire  $2\pi$  steradian envelope centered about the direction of light travel.

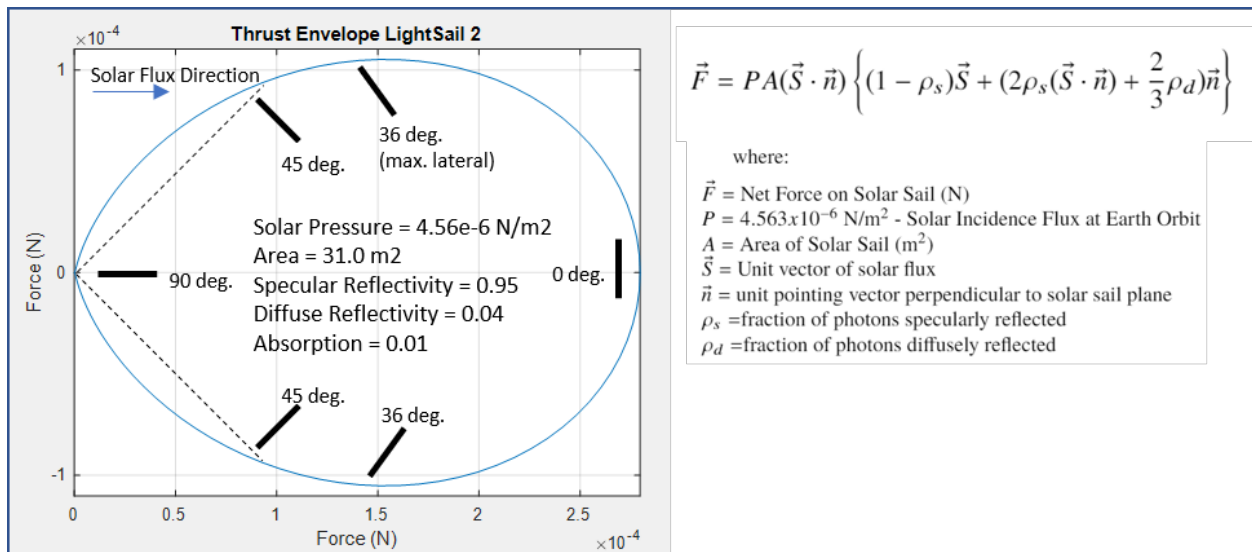


**Fig. 4 An overview of the physics and acceleration capabilities of a solar sailing spacecraft**

Figure 4 shows the thrust envelope of a sailcraft similar to LightSail 2 and the equation describing the force output as a function of sail angle and reflectivity. The PID controller implemented in figure 3 is then adapted to a solar sailing spacecraft by adapting the acceleration commands to what is actually possible via sail orientation. If the direction of the acceleration command is within  $\pi/2$  of the solar flux, then the solar sail is oriented to give whatever thrust it can in that direction, up to the total acceleration commanded (It is assumed that the solar sail can be throttled back via reorienting to be perpendicular to the sun when the required delta-V from an acceleration command is exceeded).

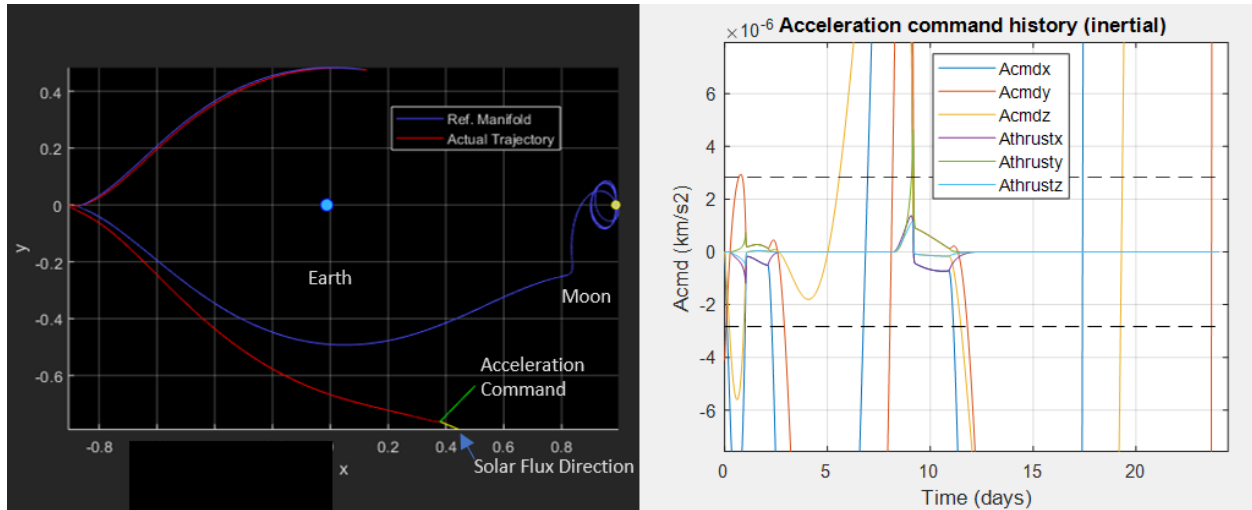


**Fig. 5 Direct adaptation of the PID controller to the solar sail produces poor trajectory control**

If the commanded acceleration is against the direction of the solar flux, then the solar sail is oriented perpendicular to the sun's rays, resulting in zero thrust. The concept is that since the orientation of the solar flux (as seen from the rotating earth-moon frame) will rotate through a full circle every 27 days, this will provide enough variation so that 3d control can be effectively exercised. Figure 5 shows the result of the experiment, with the actual thrust only being used for a small fraction of the 24 day propagation, and the resulting position error significant and diverging at the end of the trajectory. Clearly additional measures are required to stabilize the flight path.

### C. Trajectory Biasing

Improved performance can be obtained by theoretically biasing the reference manifold trajectory as shown in figure 6. Here, a position offset to the reference trajectory is calculated such that a restoring acceleration is directly towards the sun. The concept is that by biasing in this manner, we can establish a trajectory into which the commanded acceleration is biased into the center of the solar sail spacecraft capability.

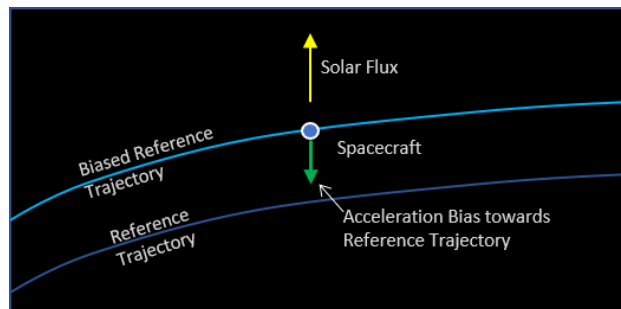


**Fig. 6 Differential position analysis leads to position offsets which accelerate in direct opposition to the sun, biasing the trajectory into an area where the solar sail can provide full three axis control**

In practice, this effect helps, but does not prove to completely solve the problem. The resulting biased trajectory is not constant with time, but moves as a result both of the changing solar flux direction and orbital dynamics. Although

one might expect that biasing the trajectory so that accelerations are in the center of the spacecraft's capability, this produces an offset which moves dynamically on its own accord which proves too difficult for the spacecraft to follow. However, modest improvements to performance can be obtained with modes reference trajectory biases of approximately 5 percent of the total acceleration capacity, and this improvement is shown in figure 6. Larger offsets prove to have poorer performance.

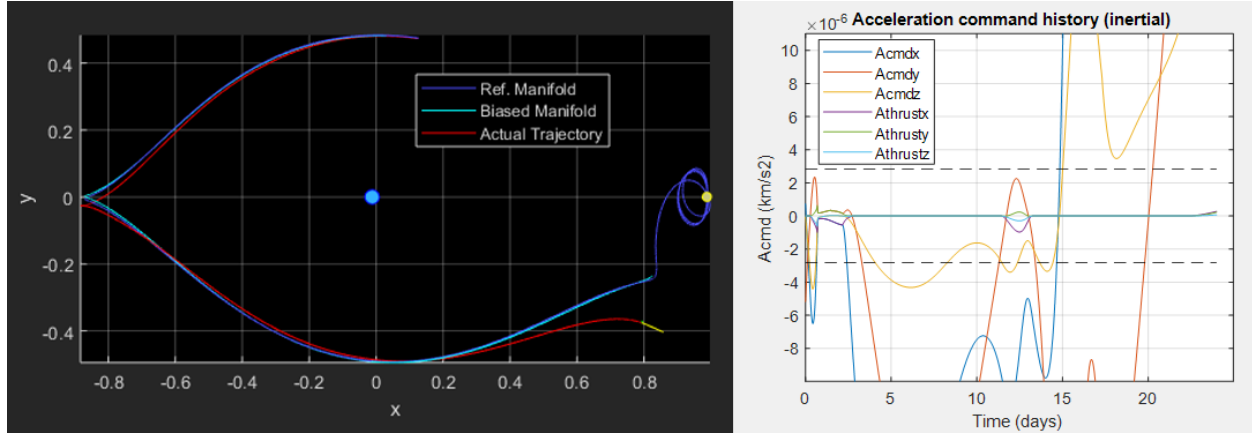


**Fig. 7 Biasing the baseline manifold against the solar flux significantly improves performance**

#### IV. Summary

In summary, although results are encouraging more work remains to be done to establish a practical solar sailcraft control algorithm to both reach the entry point for a halo trajectory manifold, as well as maintaining position once on the manifold. It is plausible that performance could be improved via establishment of manifolds for the real-world 4 body problem, and other techniques, such as genetic algorithms could establish trajectory control where much of the time the spacecraft is coasting, awaiting rotation of the solar flux vector to a useful orientation. Finally, the insertion of the spacecraft into the reference manifold appears to take about 100m/s of delta-V and this provides a significant challenge to the acceleration capacity of a solar sail spacecraft without the significant improvements to acceleration performance which are assumed in this paper.

#### Acknowledgments

The authors would like to thank Dr. Eric Butcher at the University of Arizona for his teaching and tutorship regarding interplanetary mission design and halo orbits.

#### References

- [1] Vallado, D., *Fundamentals of Astrodynamics and Applications*, 2013.
- [2] Howell, K. C., "Three-dimensional, periodic, 'halo' orbits," *Celestial mechanics*, Vol. 32, No. 1, 1984, pp. 53–71.
- [3] Anthony, W., Larsen, A., and Butcher, E., "Optimal impulsive manifold-based transfers with guidance to Earth-Moon L1 halo orbits," *23rd AAS/AIAA Space Flight Mechanics Meeting, Spaceflight Mechanics 2013*, Univelt Inc., 2013, pp. 2093–2112.
- [4] Daniel, J. G., "Generating Periodic Orbits in the Circular Restricted Three-Body Problem with Applications to Lunar South Pole Coverage," Ph.D. thesis, Ms dissertation, Purdue University, West Lafayette, Indiana, 2006.
- [5] Nallapu, R., Vance, L. D., and Thangavelautham, J., "Automated Design Architecture for Lunar Constellations," *2020 IEEE Aerospace Conference Proceedings*, IEEE, 2020.
- [6] Davis, K., Parker, J., and Butcher, E., "Transfers from Earth to Earth–Moon L3 halo orbits using accelerated manifolds," *Advances in Space Research*, Vol. 55, No. 7, 2015, pp. 1868–1877.
- [7] Das, A., "Solar sail trajectory design in the Earth-Moon circular restricted three body problem," 2014.